

An Autocorrelation Modeling Method for Oxygen Saturation Measurement During Low Perfusion

Shuangping Tan (✉ tanshuangpingzy@163.com)

The Jiangxia District No.1 People's Hospital of Wuhan, Wuhan, 430200

Jie Wei

The Jiangxia District No.1 People's Hospital of Wuhan, Wuhan, 430200

Hao Chen

The Jiangxia District No.1 People's Hospital of Wuhan, Wuhan, 430200

Tong Zhang

State Key Laboratory of Information Engineering in Surveying, Mapping and Remote Sensing, Wuhan University, Wuhan, 430079

Xiali Wu

The Jiangxia District No.1 People's Hospital of Wuhan, Wuhan, 430200

Youfeng Deng

The Jiangxia District No.1 People's Hospital of Wuhan, Wuhan, 430200

Hongbin Zuo

The Jiangxia District No.1 People's Hospital of Wuhan, Wuhan, 430200

Research Article

Keywords: Pulse oximetry, SpO₂ extraction, Low perfusion, Autocorrelation modeling method

Posted Date: January 23rd, 2021

DOI: <https://doi.org/10.21203/rs.3.rs-150041/v1>

License:  This work is licensed under a Creative Commons Attribution 4.0 International License.

[Read Full License](#)

1 **An autocorrelation modeling method for oxygen**
2 **saturation measurement during low perfusion**

3 Tan Shuangping*^{#1}, Wei Jie*¹, Chen Hao*¹, Zhang Tong², Wu Xiali¹, Deng Youfeng¹,
4 Zuo Hongbin^{#1}

5 * These authors contribute equally to this work

6 # Correspondence: tanshuangpingzy@163.com

7 Affiliation:

8 1. The Jiangxia District No.1 People's Hospital of Wuhan, Wuhan, 430200, China

9 2. State Key Laboratory of Information Engineering in Surveying, Mapping and Remote
10 Sensing, Wuhan University, Wuhan, 430079, China

11

12 **Abstract:**

13 Background: SpO₂ is a widely used estimation of oxygen saturation owing to its
14 convenient usage and low cost. However, SpO₂ determination under low perfusion
15 condition is severely affected by noise.

16 Methods: In this paper, an autocorrelation modeling method for the oxygen saturation
17 measurement during low perfusion is presented. The proposed method mainly contains
18 two steps: calculating the autocorrelation of the photoplethysmography (PPG) signals and
19 modeling for the parameter calculation. The autocorrelation of the PPG signals can
20 suppress the noise and extract pulse waves from low perfusion signals. The model can
21 realize the calculation of SpO₂ with the autocorrelation signals.

22 Results: Experiments showed that the new method had a good accuracy and stability
23 under low perfusion condition (perfusion index (PI)≤0.2%), and it was also motion-

24 tolerant. Meanwhile, the new method showed a good performance for the oxygen
25 saturation measurement under the condition of lower perfusion($PI=0.1\%$).

26 Conclusions: The new method could realize the calculation of SpO_2 by little computation
27 and high efficiency without extra hardware. It has strong potential in real-time clinical
28 use.

29 **Keywords:** Pulse oximetry, SpO_2 extraction, Low perfusion, Autocorrelation modeling
30 method

31

32 **1 Background**

33 Saturation of peripheral oxygen (SpO_2), which reflects arterial oxygenation levels, is often
34 used to assess the function of the respiratory system and the circulation system. Pulse
35 oximetry is a non-invasive technique, recording from extremities such as fingers and ear
36 lobes, to continuously monitor SpO_2 . Owing to its cost-effectiveness benefits, pulse
37 oximetry has become a regular monitoring device used in anesthesia, surgical operation,
38 and intensive care^[1,2]. However, clinical applications of pulse oximetry revealed that the
39 measurement accuracy and precision were severely affected by motion and low peripheral
40 perfusion caused by low ambient temperature or cardiogenic shock^[3,4]. In case of low
41 perfusion, the amplitude of photoplethysmography (PPG) signals, which is used to
42 calculate SpO_2 , become very small and hidden in noise. The signal-to-noise ratio (SNR) is
43 too low to extract useful information with conventional methods(Fig. 1 b). In case of
44 motion, PPG signals are contaminated by motion artifacts. The frequency spectrum
45 overlap of PPG signals with motion artifacts makes conventional low-pass or high-pass
46 filter techniques inapplicable. Therefore, new methods are needed to deal with the issue
47 mentioned above.

48 To overcome the shortcomings of motion and low perfusion, many algorithms were
49 developed in the past few years. For instance, Masimo Corporation proposed Discrete
50 Saturation Transform (DST) method to adaptively filter out noise from recordings by
51 constructing a reference noise ^[5]. Yan et al. proposed a robust minimum correlation
52 discrete saturation transform (MCDST) algorithm to remove motion artifact ^[6]. Yousefi et
53 al. developed a real-time adaptive algorithm to extract heart rate and SpO₂ for a wireless
54 pulse oximeter allowing users to move freely ^[7]. Byung et al. proposed independent
55 component analysis to reduce noise in PPG signals^[8]. However, this method did not
56 perform well for low perfusion interference. Foo proposed two algorithms to account for
57 the difference between the properties of low perfusion signal and motion contaminated
58 PPG ^[9]. However, Foo's method for low perfusion case was a complicated non-causal
59 filter technique commonly used for off-line analysis. In addition, SpO₂ was not extracted
60 in their work. Therefore, new algorithms for accurately extracting SpO₂ under low
61 perfusion is required, especially for the anesthesia, surgical operation, and intensive care
62 application.

63 Here we propose a novel autocorrelation modeling method for determining SpO₂ under
64 low perfusion conditions. First, we characterize the properties of PPG
65 (photoplethysmography) signals under low perfusion condition. Then, we deduce the new
66 autocorrelation based SpO₂ extraction method. At last, validation test results of the
67 method on accuracy, stability, and motion-tolerance are presented. The new SpO₂
68 extraction method have potential of real-time clinical use.

69 **2 Methods**

70 To realize the accurate measurement of SpO₂ under low perfusion condition, we
71 designed a pulse oximetry to acquire PPG signals(generated by a SpO₂ simulator-Fluke
72 Index 2XL) which are pre-processed and used for calculating the alternative

73 component(AC) and the direct component(DC). We computed autocorrelation on
74 recorded AC signals, then calculated the SpO₂ with the autocorrelation preprocessed
75 signals by our modeled method. The overall process is shown in Fig. 2.

76 **2.1 PPG signal generation**

77 Photoplethysmography (PPG) signals, which are used to extract SpO₂, can be obtained
78 when illuminating the body with a light beam at a haemoglobin-sensitive wavelength. In
79 the peripheral sites to be recorded, the volume of blood within the illuminating field alters
80 periodically to the artery pulsation, thus generating fluctuating PPG signals. A PPG signal
81 can be represented as an addition of an alternative component (AC) and a direct
82 component (DC). The DC signals reflect lights that are absorbed or scattered by vein, base
83 volume of artery, and other non-pulsatile tissue, while the AC signals reflect volume
84 change in the artery and arterial blood. The parameter PI (perfusion index) is an indication
85 of the peripheral perfusion level, which can be simply calculated by the ratio of AC to DC
86 amplitude($PI=P_{AC}/P_{DC}$). In the low perfusion case, PI can be less than 0.2%.

87 To develop the new method, two kinds of PPG signals were used: 1) simulated signals,
88 and 2) recorded signals. A way to model low perfusion condition is lowering the
89 peripheral temperature. However, its controllability and reproducibility are relatively low.
90 Therefore, we used simulated PPG signals generated by a SpO₂ simulator-Fluke Index
91 2XL (Fluke Biomedical, USA). With the simulator, we could obtain PPG signals with
92 preset PI₂ (PI for infrared case), PR (pulse rate), and SpO₂ (Fig. 1). Signal simulation is a
93 good tool for developing and testing the new method for low perfusion case. On the other
94 hand, motion artifacts were modeled by direct recording the PPG as the users moved their
95 fingers. A home-made reusable dual-wavelength PPG sensors were used in this case.

96 2.2 Calculation of SpO₂

97 2.2.1 Principle of SpO₂ extraction

98 Oxygen saturation can be calculated by concentration of oxyhaemoglobin (HbO₂) and that
99 of deoxyhaemoglobin (Hb). Since the absorption spectra of HbO₂ and Hb are different in
100 the red and infra-red regions, two monochromatic lights are commonly used to illuminate
101 peripheral vascular bed. Two PPG signals and two PIs are formed based on light
102 transmission. Therefore, SpO₂ can be calculated according to Beer-Lambert Law as
103 follows:

$$104 \quad SpO_2 = \frac{\epsilon_{Hb}^{\lambda_2} R - \epsilon_{Hb}^{\lambda_1}}{(\epsilon_{HbO_2}^{\lambda_1} - \epsilon_{Hb}^{\lambda_1}) - (\epsilon_{HbO_2}^{\lambda_2} - \epsilon_{Hb}^{\lambda_2}) R} \quad (1)$$

105 Where, λ_1 and λ_2 are the two wavelengths (in 660 and 940 nm); R is the ratio of the two
106 PIs (i.e., $R=PI_1/PI_2$); $\epsilon_{HbO_2}^{\lambda_1}$ and $\epsilon_{HbO_2}^{\lambda_2}$ are the extinction coefficients of HbO₂ at λ_1 and
107 λ_2 ; $\epsilon_{Hb}^{\lambda_1}$ and $\epsilon_{Hb}^{\lambda_2}$ are the extinction coefficients of Hb at λ_1 and λ_2 . All the relevant
108 coefficients are constant^[10]. Therefore, SpO₂ is determined as R is obtained from
109 recordings. Considering individual differences in scattering effect and other uncertainty
110 factors, Eq.1 is generally expanded in terms of second-order Taylor series in practice as
111 follows:

$$112 \quad SpO_2 = A * R^2 + B * R + C \quad (2)$$

113 Where the coefficients A , B , and C can be calibrated by fitting the data to a conic curve
114 using Least Squares.

115 2.2.2 Principle of autocorrelation modeling

116 Autocorrelation modeling consists of 1) autocorrelation function computation, and 2)
117 relating SpO₂ and other parameters to autocorrelation signals. Before going into the
118 autocorrelation modeling details, we review the autocorrelation technique first.

119 Autocorrelation technique is a weak signal detection technique, particularly for signals
120 with cyclic properties, such as ECG. For a signal $x(t)$, and its autocorrelation function is
121 defined as

$$122 \quad R_x(\tau) = \lim_{T \rightarrow \infty} \frac{1}{T} \int_0^T x(t)x(t+\tau)dt \quad (3)$$

123 Now, we present a simple demonstration of noise reduction of autocorrelation
124 technique. Given a sinusoidal signal $s(t)=A\sin(\omega t+\varphi)$ and its noise $n(t)$, the signal $x(t)$ is a
125 sum of these two signals; i.e., $x(t)=s(t)+n(t)=A\sin(\omega t+\varphi)+n(t)$. Then, the autocorrelation
126 function of this signal is

$$\begin{aligned} 127 \quad R_x(\tau) &= \lim_{T \rightarrow \infty} \int_0^T [s(t) + n(t)][s(t+\tau) + n(t+\tau)]dt \\ &= \lim_{T \rightarrow \infty} \int_0^T s(t)s(t+\tau)dt + \lim_{T \rightarrow \infty} \int_0^T s(t)n(t+\tau)dt \\ &\quad + \lim_{T \rightarrow \infty} \int_0^T n(t)s(t+\tau)dt + \lim_{T \rightarrow \infty} \int_0^T n(t)n(t+\tau)dt \\ &= R_s(\tau) + R_{sn}(\tau) + R_{ns}(\tau) + R_n(\tau) \end{aligned} \quad (4)$$

128 Since the original signal $s(t)$ and its noise $n(t)$ are independent, and if the noise is white
129 noise, the three latter terms tend to be zero as $\tau \rightarrow \infty$. Thus we have

$$130 \quad R_x(\tau) = R_s(\tau) = \frac{A^2}{2} \cos \omega \tau \quad (5)$$

131 The autocorrelation function has the same frequency to the original signal, and the
132 amplitude can be related to that of the original. Therefore, useful information can be
133 extracted while noises are reduced^[11,12].

134 *2.2.3 Autocorrelation modeling of SpO₂*

135 PPG signals, are regenerative and can be regarded as cyclic in a small period of time.

136 Suppose the resolved AC component of PPG is denoted by $p_{AC}(t)$, then we have

137
$$p_{AC}(t) = p_{AC}(t + mT) = P_{AC} \cdot g_{AC}(t) \quad (6)$$

138 Where T is the period of $p_{AC}(t)$; m is an arbitrary constant; $g_{AC}(t)$ is normalized $p_{AC}(t)$,

139 and P_{AC} is the amplitude of $p_{AC}(t)$. Recall that SpO₂ is calculated from R , which is the

140 ratio of the two PIs. Since PI is defined as the ratio of AC and DC amplitude,

141 conventional computation of R is as follows:

142
$$R = \frac{PI_1}{PI_2} = \frac{P_{AC1}/P_{DC1}}{P_{AC2}/P_{DC2}} = \frac{P_{AC1}/P_{AC2}}{P_{DC1}/P_{DC2}} \quad (7)$$

143 However, in the low perfusion case, both P_{AC1} and P_{AC2} are very weak and prone to be

144 distorted by noise and interference, while the amplitude of DC component was less

145 affected. To suppress noise, we compute autocorrelations on recorded AC signals.

146 Suppose the noise in the recorded AC signal $pr_{AC}(t)$ is denoted by $n(t)$; i.e., $pr_{AC}(t) = p_{AC}(t) + n(t)$.

147 The autocorrelation function of $pr_{AC}(t)$ can be represent as follows:

148
$$\begin{aligned} R_{pr_{AC}}(\tau) &= R_{p_{AC}}(\tau) + R_{p_{AC}n}(\tau) + R_{np_{AC}}(\tau) + R_n(\tau) \\ &= R_{p_{AC}n}(\tau) + R_n(\tau) = P'_{AC} \cdot g'_{AC}(\tau) \end{aligned} \quad (8)$$

149 Where $R_{p_{AC}n}(\tau)$ and $R_{np_{AC}}(\tau)$ are cross-correlations of $p_{AC}(t)$ and $n(t)$, which equal to zero

150 as they are independent with each other. $g'_{AC}(\tau)$ is normalized autocorrelation signals of

151 $pr_{AC}(t)$ and P'_{AC} is the amplitude of autocorrelation signals of $pr_{AC}(t)$. $R_n(\tau)$ is only non-

152 zero at $\tau=0$. Therefore, the weak cyclic pulsation signal was retrieved from the stable

153 autocorrelation function with a strongly suppressed noise. Besides, since autocorrelation

154 does not change the periodical property of the original signal, $R_{pr_{AC}}(\tau)$ is also regenerative

155 and has a period of T and has an amplitude proportional to the square of P_{AC} ; i.e.,

156
$$P_{AC} = k\sqrt{P'_{AC}} \quad (9)$$

157 Where k is the amplitude transfer factor (Fig. 3). Unlike sinusoidal signal, k does not
 158 exactly equal to $2^{1/2}$ and, in practice, we determined it empirically through experimental
 159 trials. In this way, the amplitude of AC component of the PPG signal, i.e. P_{AC} , can be
 160 determined.

161 Given P_{AC} , the perfusion index (PI) can be calculated from the amplitude of DC
 162 component (P_{DC}), which is relative easy to be determined; thus we have

163
$$PI = P_{AC}/P_{DC} = (k\sqrt{P'_{AC}})/P_{DC} \quad (10)$$

164 In the dual-wavelength method, we actually obtained two PIs corresponding to
 165 wavelength λ_1 and λ_2 , respectively. Therefore, with autocorrelation modeling method, we
 166 obtained R (denoted as R' to be distinguished from R calculated with Eq. 7) as follows:

167
$$R' = \frac{PI_1}{PI_2} = \frac{k_1\sqrt{P'_{AC1}}/k_2\sqrt{P'_{AC2}}}{P_{DC1}/P_{DC2}} \quad (11)$$

168 Where k_1 and k_2 are amplitude transfer factors at the two wavelengths. Thus we compute
 169 SpO_2 as follows:

170
$$SpO_2 = A * R'^2 + B * R' + C \quad (12)$$

171 **2.3 Implementation of SpO_2**

172 To extract SpO_2 accurately, the autocorrelation modeling technique, in practice, is
 173 comprised of four steps described as follows.

174 (1) Signal recording and pre-processing. The dual-wavelength signals were recorded
 175 and packed in a crosswise format for the convenience of data transmission. In the pre-
 176 processing step, data from the same source would be accumulated in a dedicated data pool

177 for later use. After data-rearrangement, the raw data were low-pass filtered to reduce
178 noise, notch filtered to suppress power-line interference.

179 (2) P_{AC} and P_{DC} computation. As for P_{DC} , the computation was relatively simple: low-
180 pass filtering the raw data and calculating the mean value. As for P_{AC} , we high-pass
181 filtered the original PPG AC signal and computed the difference between peak and valley.

182 (3) Computation of autocorrelation function and its amplitude. In practice, the
183 summation limit to calculate autocorrelation function can never be infinite and should be
184 truncated:

$$185 \quad R_x(m) = \frac{1}{N} \sum_{n=0}^{N-1-|m|} x(n)x(n+m) \quad (13)$$

186 Where, $N \gg m$. The fast computation of autocorrelation is generally achieved by FFT and
187 window technique. To make the method be adaptive to real-time use, we employed the
188 circular autocorrelation technique (Supplementary Fig. 1). Suppose the length of the data
189 pool is N , the length of autocorrelation function should also be N . The tail of the pool was
190 linked to the head. In this way, when the pool was full, the algorithm turns to the head of
191 the data pool to restore and retrieve the new data. To compute the amplitude of the
192 autocorrelation function, we integrated one cycle of data.

193 (4) Computation of R' and SpO_2 according to Eqs. (9)-(12). Every 6 seconds a new set
194 of results were generated.

195 **2.4 Data analysis**

196 The new algorithm--autocorrelation modeling of SpO_2 --was carried out on Matlab
197 (MathWorks, USA). Linear regression and other statistical analysis were done by
198 OriginPro v9.0 (OriginLab, USA) and Excel (Microsoft, USA). Statistical data were
199 represented as mean \pm SD.

200 **3 Results**

201 **3.1 Autocorrelation modeling results**

202 The new autocorrelation modeling method was built based on two linearity assumptions:

203 1) the amplitude of original AC component is proportional to square root of that of
204 autocorrelation function as denoted by Eq. (9), and 2) the substitution of R with R' in Eq.
205 (2). Here, we test the two linearity assumptions.

206 First, we created PPG signals for $PI=3\%$, $PR=75$, and SpO_2 (%) ranges from 36 to 100
207 using Fluke Index. The simulated signal at each SpO_2 was recorded and transmitted to
208 PC.

209 We calculated the magnitudes of original PPG AC component (P_{AC}) and those of the
210 autocorrelation functions (P'_{AC}). Since values of P_{AC} under different SpO_2 settings are
211 different, a sweep of SpO_2 (%) from 36 to 100 yielded a sufficient multi-level coverage of
212 PPG signals. At each SpO_2 settings, we calculated P_{AC} and P'_{AC} 10 times. Linear
213 regression was conducted on means of each pair ($n = 10$). It showed a nearly perfect
214 linearity between P_{AC} and $(P'_{AC})^{1/2}$ (Pearson's $r=0.99967$, Fig. 4a). Further, the amplitude
215 transfer factor k in Eq. (9) can be calculated from the slope of the regression line. In this
216 case, the wavelength was λ_1 and $k_1=1/0.348=2.874$.

217 After computation of $k_1, k_2, P'_{AC1}, P'_{AC2}, P_{DC1}$ and P_{DC2} , we calculated R and R'
218 according to Eqs. (10) and (11). Linear regression of means of R' on those of R ($n=10$)
219 yielded a regression line with slope of 1.004 and Pearson's r of 0.9998 (Fig. 4b).

220 **3.2 Accuracy**

221 To test SpO_2 extraction accuracy of the autocorrelation modeling method, we modeled the
222 low perfusion scene by simulating PPG signals with small PI (say, $PI=0.2\%$ and 0.1%)
223 (Fig. 5). A sweep of SpO_2 (%) from 64 to 96 was generated by Fluke Index. In $PI=0.2\%$

224 cases, all the SpO₂ were accurately estimated with a high precision (SD/mean < 3%) (Fig.
225 6a, Table 1). In PI=0.1% cases, SpO₂ estimates were also accurate (SD/mean < 5%) (Fig.
226 6b, Table 1).

227 **3.3 Stability**

228 To test the stability of the autocorrelation modeling method, we continuously recorded the
229 simulated PPG signal (PI=0.2%, PR=70, SpO₂=94%) for 1 hour. The mean SpO₂ fall
230 between 92 and 96 (94.3±0.6) (Fig. 6c). Further, we calculated PR from the
231 autocorrelation function and got a stable and accurate estimation (69.99±0.04) (Fig. 6d).

232 **3.4 Motion-tolerance**

233 To test the motion-tolerance of the autocorrelation modeling technique, we recorded the
234 PPG signals of our fingers with and without shaking with our home-made dual-
235 wavelength sensor^[13]. The experiment recorded two finger shaking (about 1 to 4 seconds
236 and 9 to 11 seconds, Fig. 7a). Apparently, the PPG signals with finger shaking were
237 contaminated by interference (Fig. 7a). We calculated the autocorrelation function results
238 of the PPG signals contaminated by interference. The interference was severely
239 suppressed (Fig. 7b).

240 **4 Discussion**

241 In this paper, we have described a new SpO₂ extraction method called autocorrelation
242 modeling. It involved computation of the autocorrelation function and relating its
243 magnitude to that of the original PPG signals. Autocorrelation strongly suppressed the
244 noise and picked out the weak PPG signals under low perfusion condition. We
245 demonstrated a good linearity between the magnitude of PPG signals and the square root
246 of that of the autocorrelation function, upon which SpO₂ could be accurately extracted.

247 The validation experiments using SpO₂ simulator demonstrated the high-accuracy of the
248 method in case of low perfusion(PI=0.2%) . Besides, the application of autocorrelation
249 technique also strengthened the ability of motion-tolerance.

250 In the clinical use of pulse oximetry, the SpO₂ determination under low perfusion
251 condition caused by low ambient temperature or cardiogenic shock^[2,3] is severely affected
252 by noise. This brings a lot of trouble to clinical work, such as false decreasing of SpO₂,
253 making it important to improve the accuracy of SpO₂. Compared with the adaptive
254 method using extra hardware, like accelerators to sense the motion, the new method
255 enhances PPG signals by using its inherent cyclic properties. Since the computation of
256 autocorrelation function could be achieved by Fast Fourier Transformation (FFT), the new
257 method is suitable for real-time application with little computation and high efficiency. In
258 the future, the method needs to be further improved to adapt to the accurate measurement
259 under the condition of lower perfusion(PI=0.1%) and lower SNR, especially under the
260 condition of large motion interference.

261 **5 Conclusions**

262 We introduced a method named autocorrelation modeling to solve the issue of inaccurate
263 SpO₂ measurement under low perfusion in the clinical use. The validation experiments
264 showed the autocorrelation modeling method can strongly suppress the noise and pick out
265 the weak PPG signals under low perfusion condition. The autocorrelation modeling
266 technique showed a high accuracy of the method in case of low perfusion (PI=0.2%), and
267 also strengthened the ability of motion-tolerance. The validation experiments showed a
268 strong potential in real-time clinical use for the autocorrelation modeling method.

269

270

271 **Declarations**

272 **Declarations**

273 **Ethics approval and consent to participate:**

274 All authors and participants declare that we have read and have abided by the statement of ethical standards.

275 **Consent for publication:**

276 None of the material related to this manuscript has been published or is under consideration for publication
277 elsewhere, including the internet. All authors and participants understand that the information will be
278 published, have read this manuscript and approve to have it considered exclusively for publication in BMC
279 Medical Informatics and Decision Making.

280 **Availability of data and materials:**

281 All data generated and analysed during this study are included in this published article, and any further
282 details of this study are available from the corresponding author on reasonable request.

283 **Competing interests:**

284 All authors declare that we have no competing interests.

285 **Funding:**

286 This work was financially supported by Shenzhen Med-Link Electronics Tech Co., Ltd..

287 **Authors' contributions:**

288 Tan Shuangping designed the method described in this manuscript and designed the experiment to verify
289 the method, and was the major contributor in writing the manuscript. Wei Jie and Chen Hao analyzed and
290 interpreted the experiment data, and also contributed to the writing of the manuscript. Zhang Tong, Deng
291 Youfeng and Zuo Hongbin provided a lot of help for the experimental method and writing of this paper. Wu
292 Xiali analyzed and interpreted the experiment data. All authors read and approved the final manuscript.

293 **Acknowledgements:**

294 Not applicable.

295 **Author details:**

- 296 1. The Jiangxia District No.1 People's Hospital of Wuhan, Wuhan, 430200, China
- 297 2. State Key Laboratory of Information Engineering in Surveying, Mapping and Remote Sensing, Wuhan
298 University, Wuhan, 430079, China

299

300 **References**

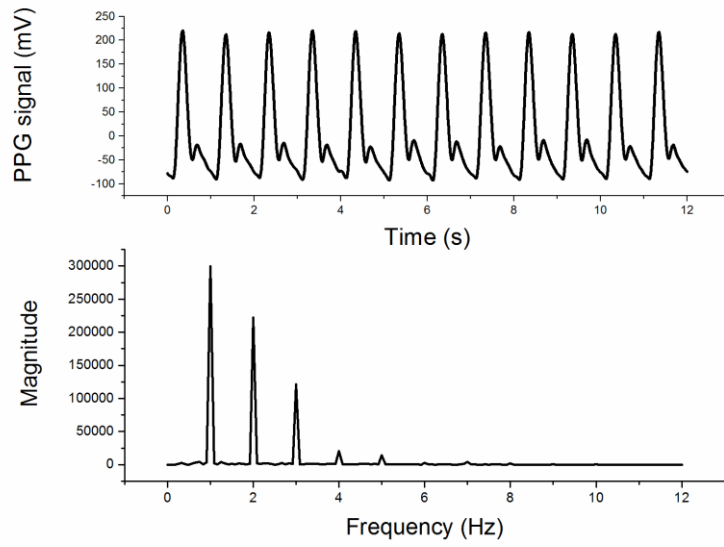
- 301 1. Docherty, Brendan. Cardiorespiratory physical assessment for the acutely ill: 2. British Journal of
302 Nursing. 2002;11: 800-807.
- 303 2. Liu Guangda, Guo Wei, Zhu Ping, Bai Mingming. Blood oxygen saturation measurement based on
304 volume signal analysis. LASER & INFRARED. 2009;02: 169-172.
- 305 3. Zhang Kun, JiaoTeng, Fu Feng, ZhangWen, Dong Xiuzhen. Motion artifact cancellation in
306 photoplethysmography using reconstruction of wavelet transform modulus maxima. Chinese Journal of
307 Scientific Instrument. 2009;3:586-589.

- 308 4. Wen Daxiang, Zhou Yin, Wang Shanjuan, Hang Yannan. The effects of motion and low perfusion on the
309 accuracy of pulse oximetry. *J Clin Anesthesiol.* 2004;06: 333-335.
- 310 5. Mohamed KD. System and methods for determining blood oxygen saturation values using complex number
311 encoding. US Patent: US7440787B2, Oct.21,2008.
- 312 6. Foo JYA, Wilson SJ. A computational system to optimise noise rejection in photoplethysmography
313 signals during motion or poor perfusion states. *Med Biol Eng Comput.* 2006;44:140-145.
- 314 7. Yousefi R , Nourani M , Ostadabbas S , Panahi I. A motion-tolerant adaptive algorithm for wearable
315 photoplethysmographic biosensors. *IEEE J Biomed Health Inform.* 2014;2:670-681.
- 316 8. Byung SK, Sun KY. Motion artifact reduction in photoplethysmography using independent component
317 analysis[J]. *IEEE Transactions on Biomedical Engineering.* 2006;3: 566-568.
- 318 9. Yan YS, Zhang YT. An efficient motion-resistant method for wearable pulse oximeter. *IEEE T Inf*
319 *Technol B.* 2008;12:399-405.
- 320 10. Yan Xinzhong, Yang Jing, Guo Lue. Study on measuring method of human oxygen saturation, medical
321 equipment. 2005;12: 1-4.
- 322 11. Chen Mingkui, Liu Zhengping .The detection of weak sinusoidal signal based on multi-layer
323 autocorrelation. *Light Industry Machinery.* 2006;3:112-115.
- 324 12. Fan Xiaozhi, Zhao Lizhi, Huang Xiaohong. An inspecting technology for weak sinusoidal signal based
325 on multi -layer autocorrelation. *Journal o f Chinese Computer Sy stems.* 2007;3: 566-568.
- 326 13. Tan S.P., Ai Z.G., Yang Y.X., Xie Q.G.. Design of a pulse oximeter used to low perfusion and low
327 oxygen saturation. *Chinese Journal of Medical Instrumentation.* 2013;37:189-196.

328

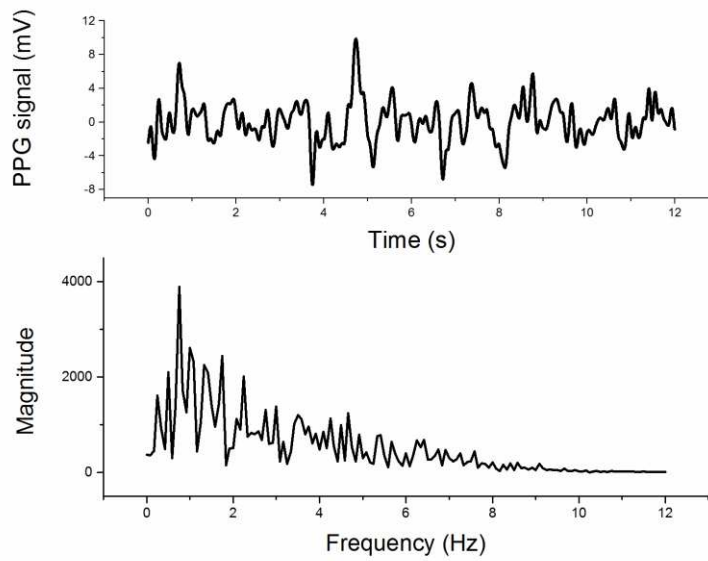
329

330 **Figures:**



331
332

(a)



333
334

(b)

335 Fig. 1 Simulated PPG signal and its Fourier spectra. (a) Normal case: $PI=3\%$, $SpO_2=96\%$, $PR=60$ times/min.
336 (b) Low perfusion case: $PI=0.075\%$, $SpO_2=96\%$, $PR=60$ times/min

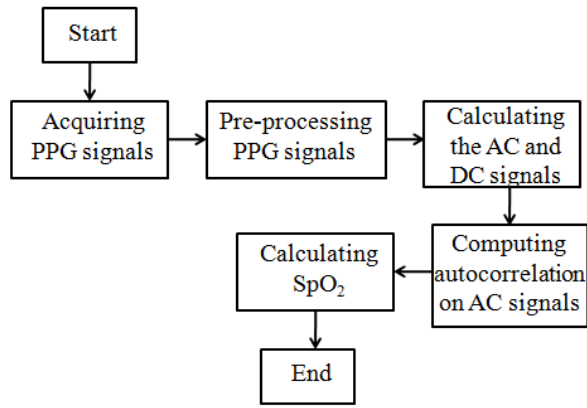


Fig. 2 Overall process of autocorrelation modeling method

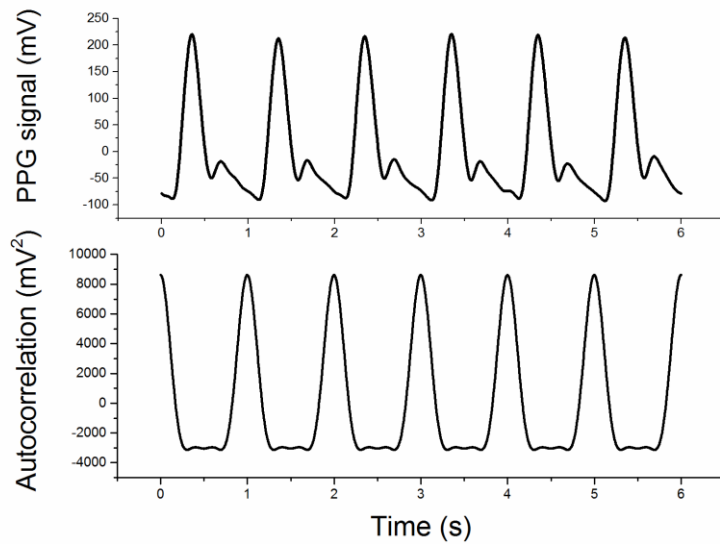
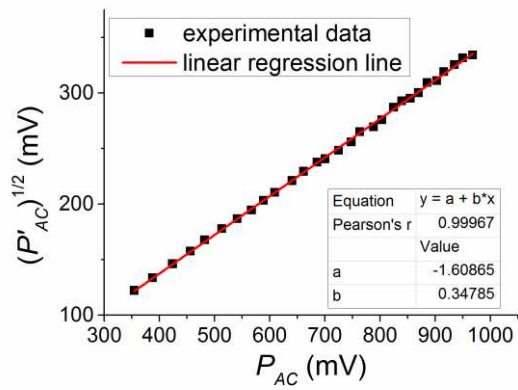


Fig. 3 Autocorrelation function of a typical normal PPG signal

337
338
339
340

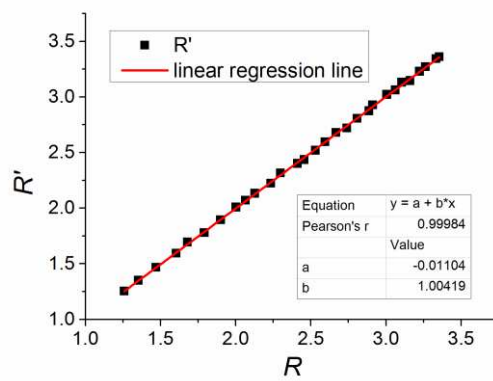
341
342
343
344
345
346



347

348

(a)



349

350

(b)

351 Fig. 4 Linear regression of the critical intermediate parameters. (a) Linear regression of square root of the

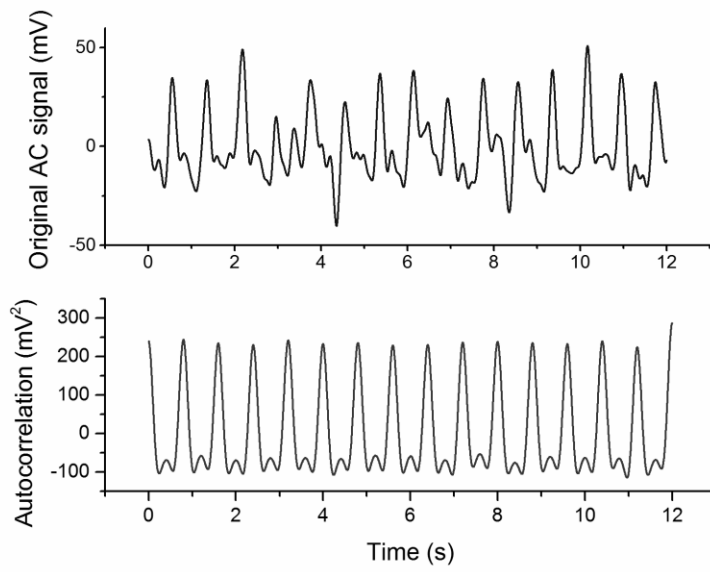
352 amplitude of autocorrelation function of PPG AC component on original PPG AC amplitude; (b) Linear

353 regression of R' on R

354

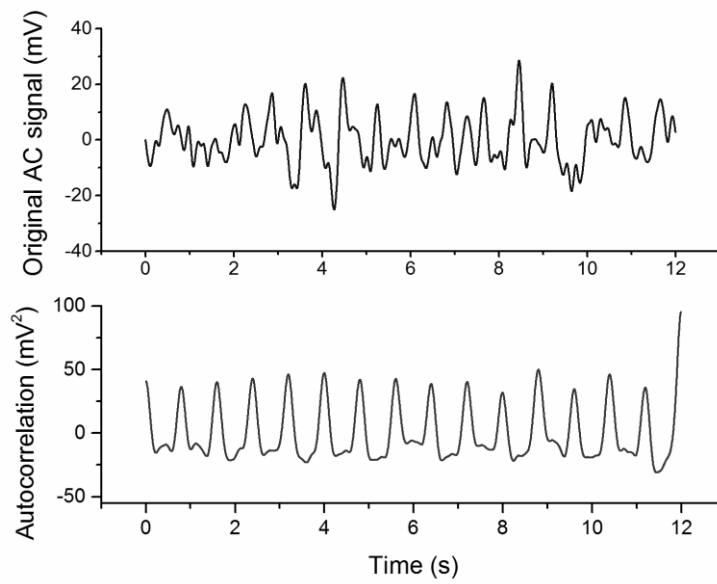
355

356



357
358

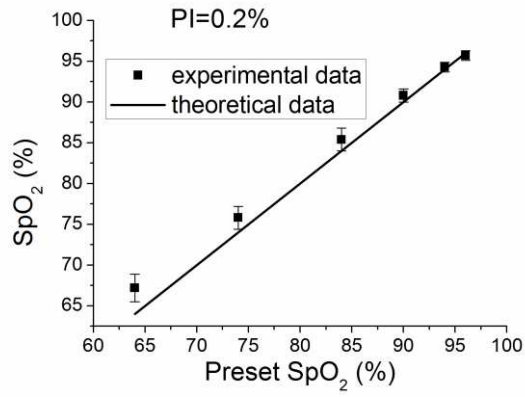
(a)



359
360

(b)

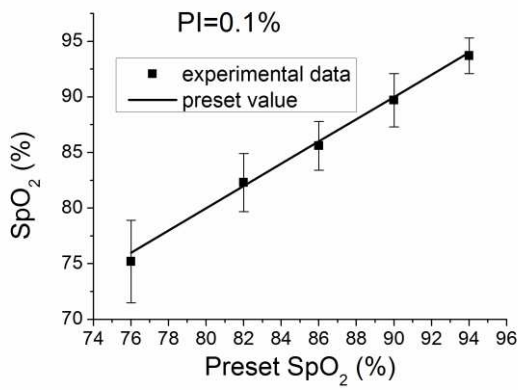
361 Fig. 5 Simulated PPG AC signal under low perfusion condition and its autocorrelation function. (a)
362 PI=0.2%; (b) PI=0.1%



363

364

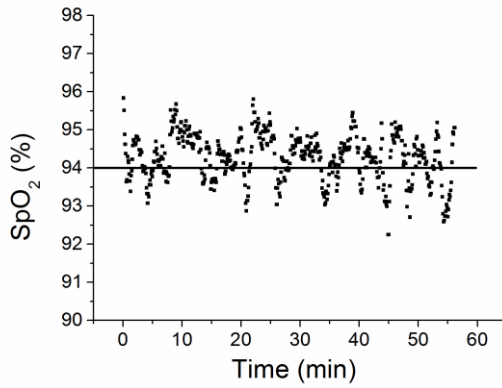
(a)



365

366

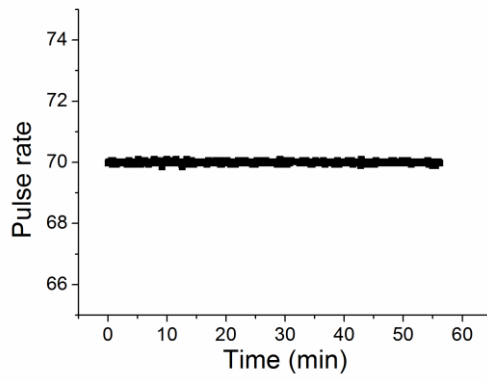
(b)



367

368

(c)



369

370

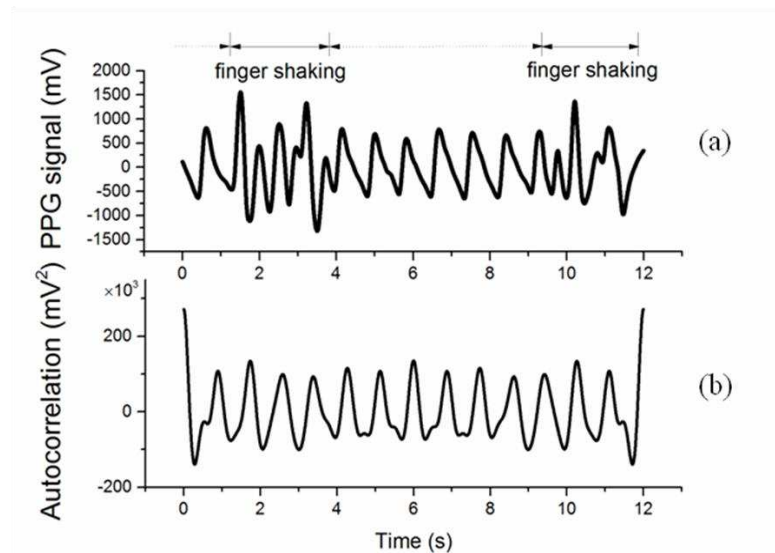
(d)

371

Fig. 6 SpO₂ and PR extracted using autocorrelation modeling method

372

373

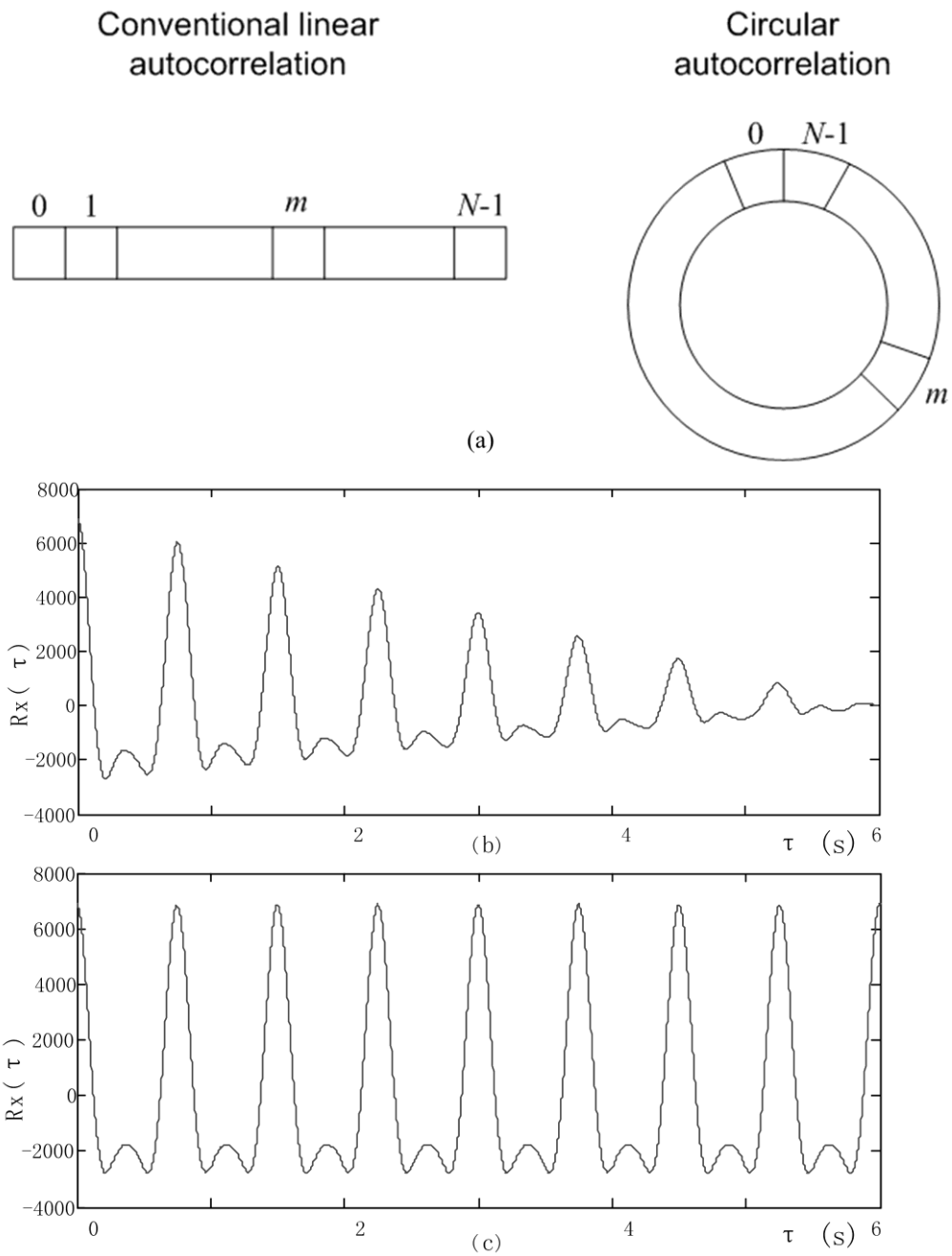


374

375

376

Fig. 7 Recorded PPG signal in case of body movement



377

378 Supplementary fig. 1 (a) Memory management of conventional linear autocorrelation and
 379 circular autocorrelation computation. (b) Autocorrelation function of a typical PPG signal
 380 calculated by conventional linear autocorrelation. (c) Autocorrelation function calculated
 381 by circular autocorrelation

382

383

384

385

386

387

388

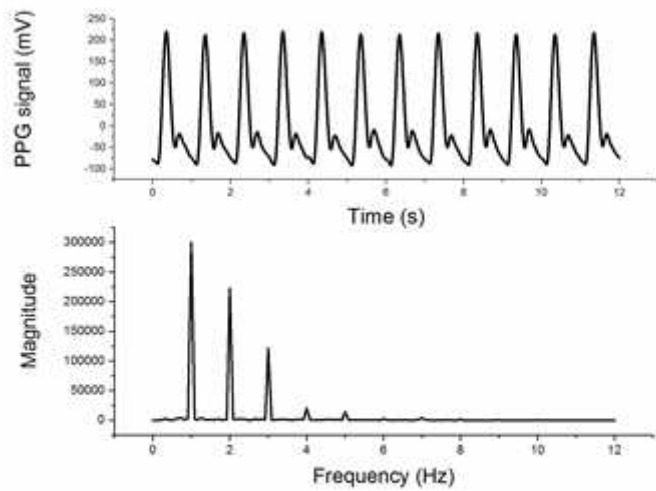
389 **Tables:**

390 Table 1 SpO₂ estimates under low perfusion condition

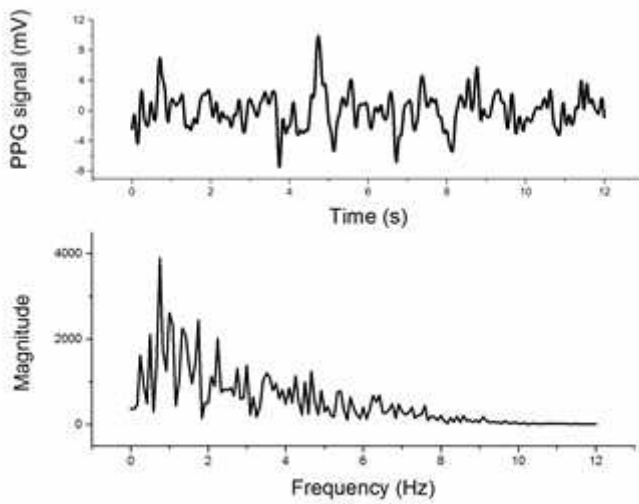
Preset SpO ₂ (%)	PI=0.2%						PI=0.1%				
	64	74	84	90	94	96	76	82	86	90	94
Mean of estimates	67.2	75.8	85.4	90.8	94.3	95.7	75.2	82.3	85.6	89.7	93.7
SD of estimates	1.7	1.4	1.4	0.8	0.6	0.6	3.7	2.6	2.2	2.4	1.6

391

Figures



(a)



(b)

Figure 1

Simulated PPG signal and its Fourier spectra. (a) Normal case: $PI=3\%$, $SpO_2=96\%$, $PR=60$ times/min. (b) Low perfusion case: $PI=0.075\%$, $SpO_2=96\%$, $PR=60$ times/min

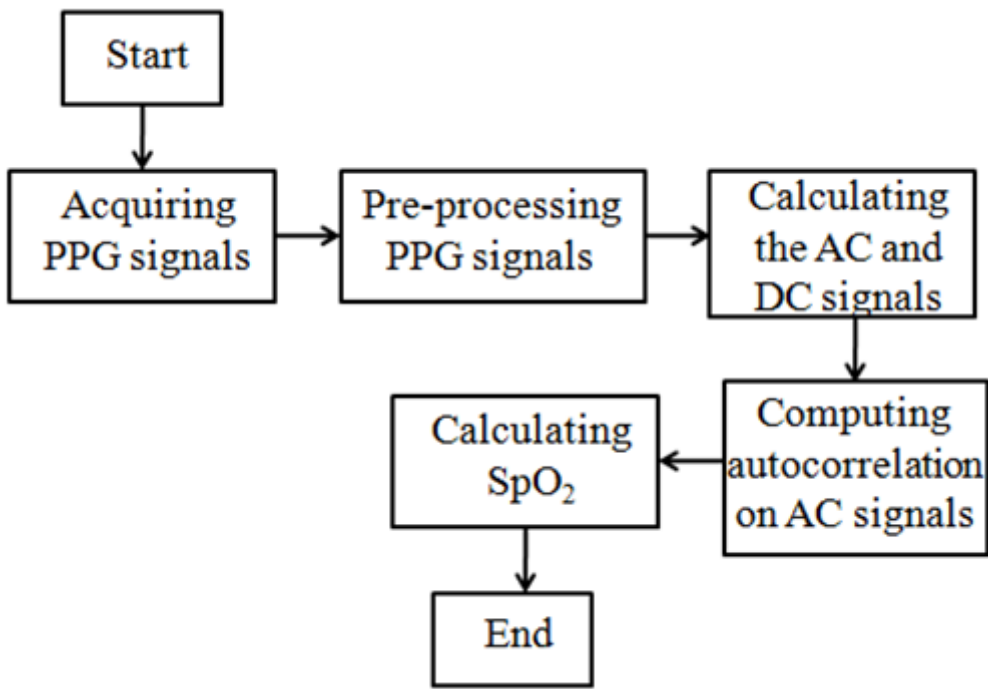


Figure 2

Overall process of autocorrelation modeling method

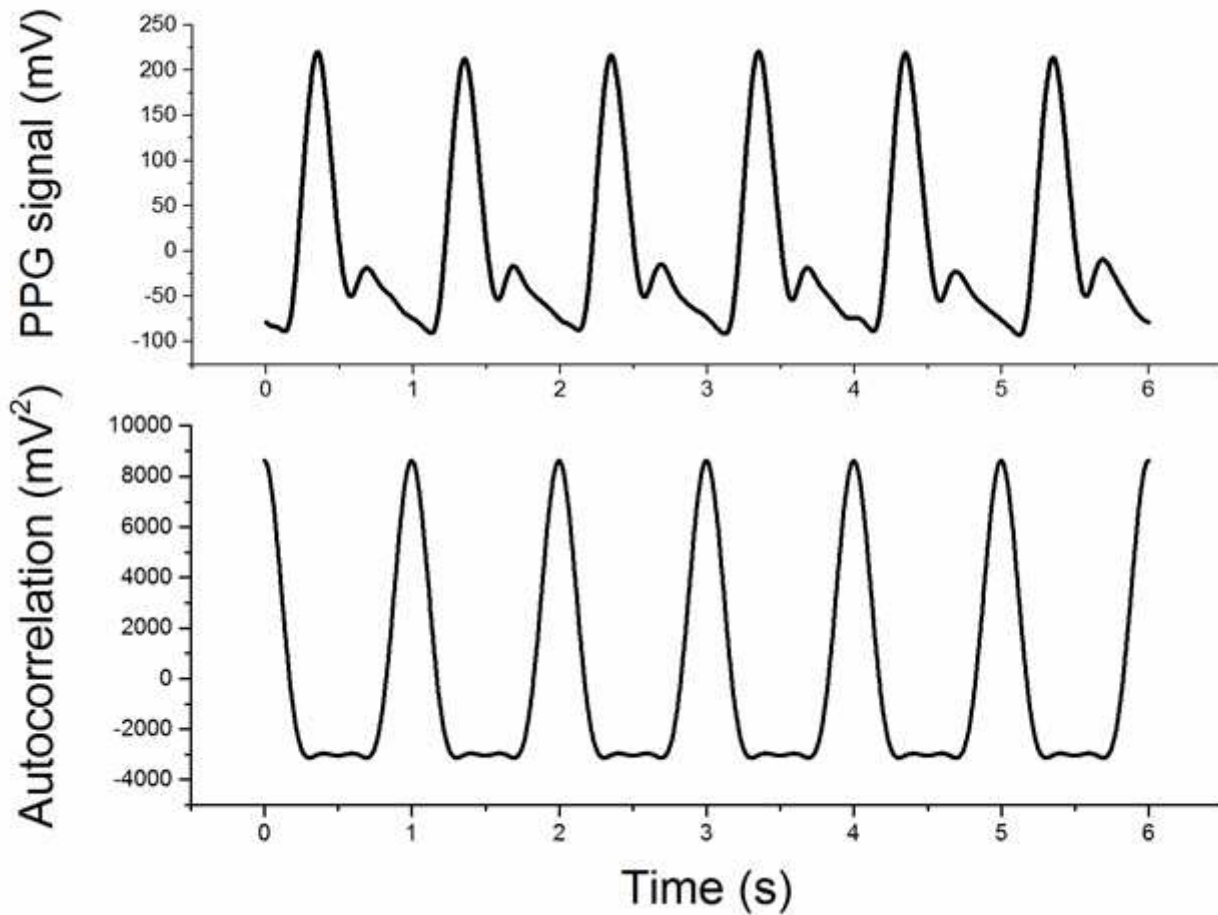
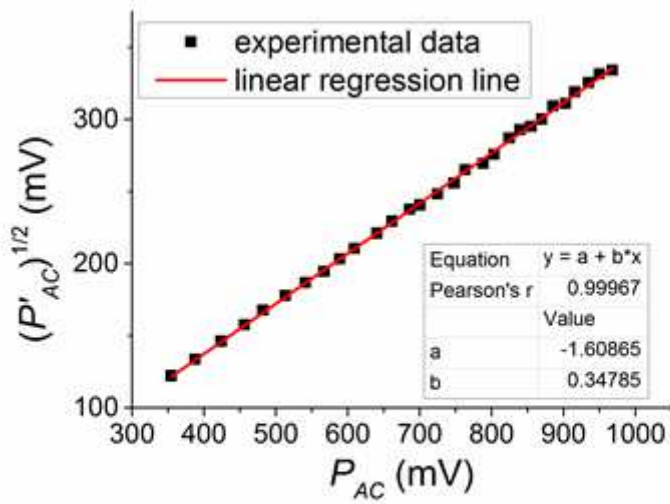
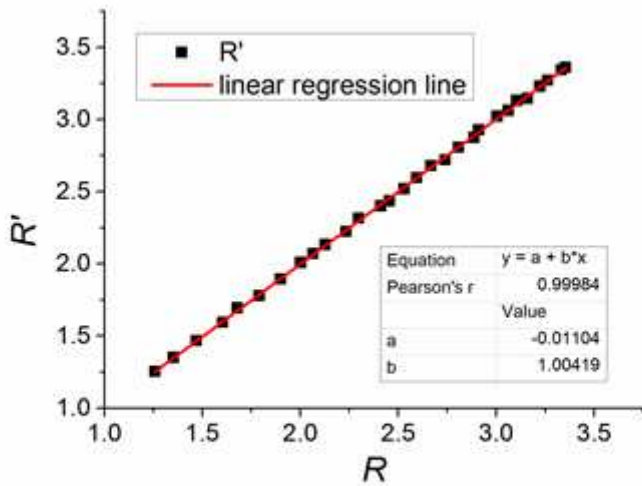


Figure 3

Autocorrelation function of a typical normal PPG signal



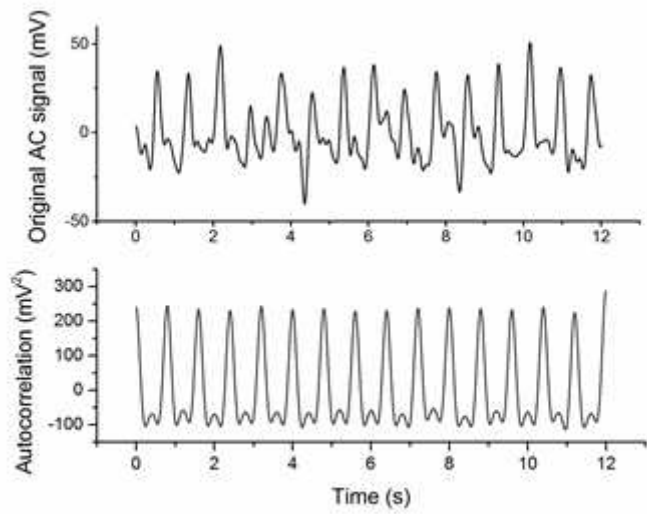
(a)



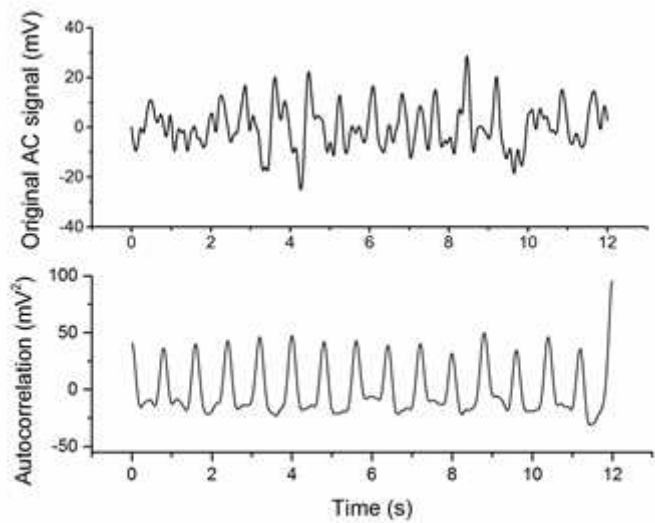
(b)

Figure 4

Linear regression of the critical intermediate parameters. (a) Linear regression of square root of the amplitude of autocorrelation function of PPG AC component on original PPG AC amplitude; (b) Linear regression of R' on R



(a)



(b)

Figure 5

Simulated PPG AC signal under low perfusion condition and its autocorrelation function. (a) $PI=0.2\%$; (b) $PI=0.1\%$

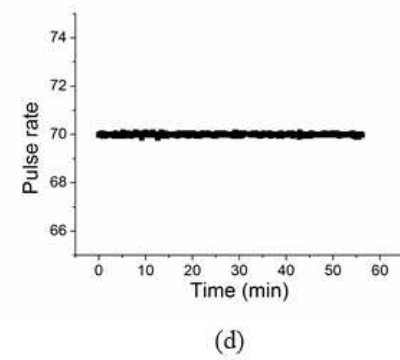
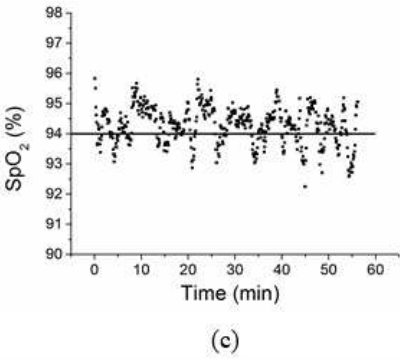
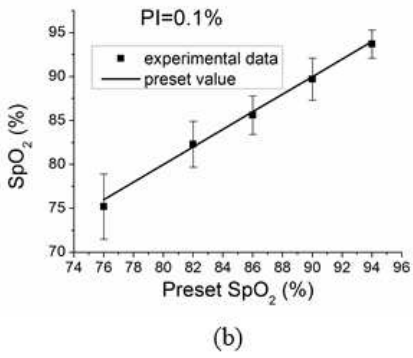
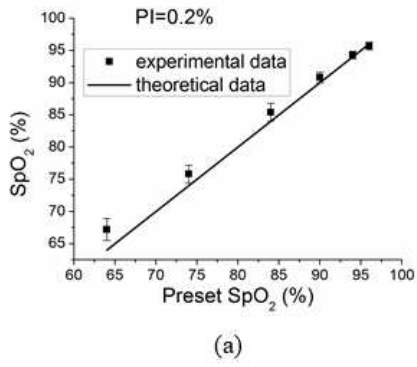


Figure 6

SpO₂ and PR extracted using autocorrelation modeling method

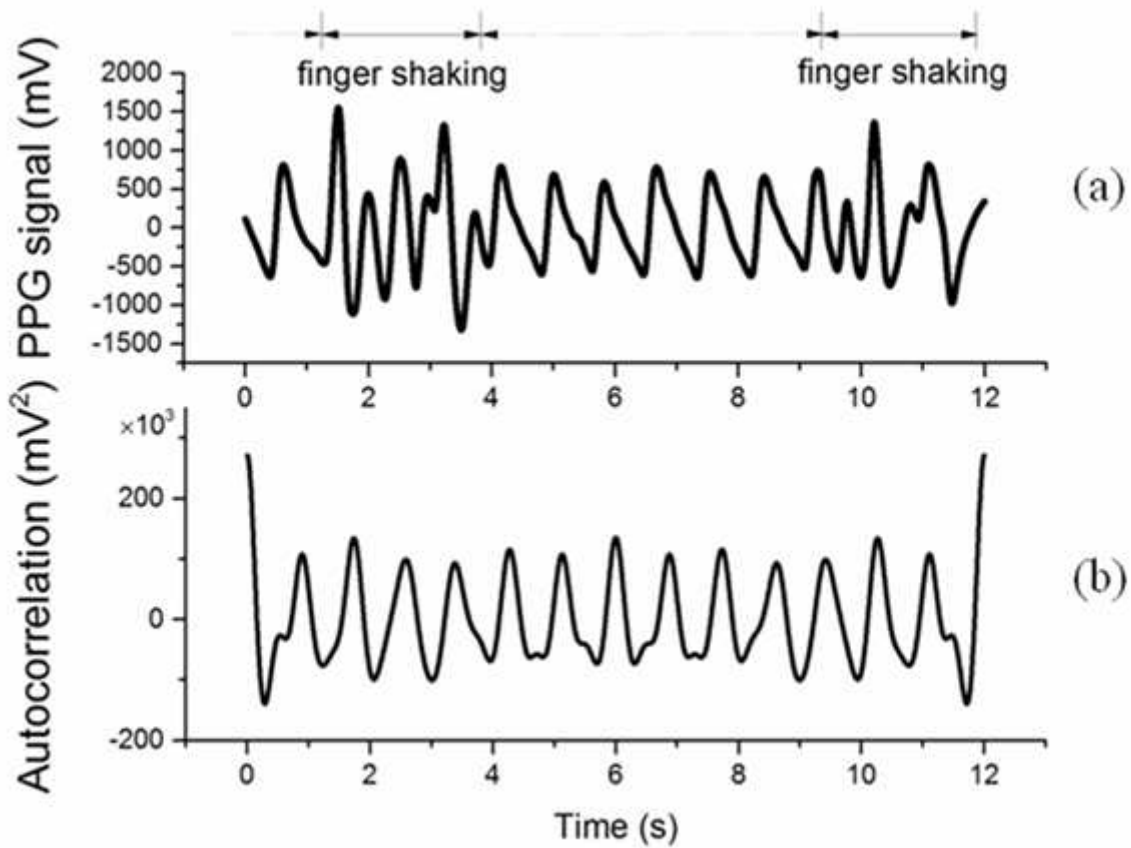


Figure 7

Recorded PPG signal in case of body movement

Supplementary Files

This is a list of supplementary files associated with this preprint. Click to download.

- [Supplementary.docx](#)